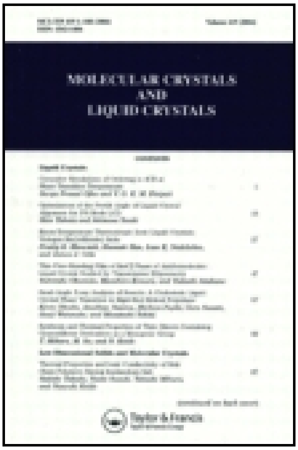

Molecular Crystals and Liquid Crystals
Publication details, including instructions for authors and subscription information:
http://www.tandfonline.com/loi/gmcl20

Quantum Efficiency of Photogeneration in Discotic Liquid Crystals: Part 1: Temperature and Wavelength Dependence

K. Scott [a], K. J. Donovan [a], T. Kreouzis [a], J. C. Bunning [a], R. J. Bushby [b], N. Boden [b] & O. R. Lozman [b]

[a] Physics Department, Queen Mary University of London, Mile End Road, London, E1 4NS, UK

[b] SOMS Centre, University of Leeds, Leeds, LS2 9JT, UK

Version of record first published: 18 Oct 2010

To cite this article: K. Scott, K. J. Donovan, T. Kreouzis, J. C. Bunning, R. J. Bushby, N. Boden & O. R. Lozman (2003): Quantum Efficiency of Photogeneration in Discotic Liquid Crystals: Part 1: Temperature and Wavelength Dependence, Molecular Crystals and Liquid Crystals, 397:1, 253-261

To link to this article: http://dx.doi.org/10.1080/714965610

Mol. Cryst. Liq. Cryst., Vol. 397, pp. 253/[553]–261/[561], 2003
Copyright © Taylor & Francis Inc.
ISSN: 1542-1406 print/1563-5287 online
DOI: 10.1080/15421400390214185

QUANTUM EFFICIENCY OF PHOTOGENERATION IN DISCOTIC LIQUID CRYSTALS: PART 1: TEMPERATURE AND WAVELENGTH DEPENDENCE

K. Scott, K. J. Donovan, T. Kreouzis, and J. C. Bunning*
Physics Department, Queen Mary University of London, Mile End Road, London E1 4NS, UK

R. J. Bushby, N. Boden, and O. R. Lozman
SOMS Centre, University of Leeds, Leeds, LS2 9JT, UK

Photocarrier generation quantum efficiencies of columnar discotic liquid crystals are determined using DC photoconduction. Photoaction spectra, of single triphenylene and binary systems comprising 50:50 stoichmetric mixtures of triphenylene with a larger triphenylene based macrocycle, demonstrate that the main generation process is due to the excitation of the smaller triphenylene molecule. Other transient photoconduction experiments have shown that carriers trap in the crystalline phase of the single systems while time of flight signals are obtained in the mesophase. Temperature dependence experiments allow carrier range to be determined in the crystalline phase for the single material and demonstrate that charge transits the binary system in both the mesophase and glassy phase.

Keywords: DC photoconduction; quantum efficiency; discotic liquid crystals; photoaction spectra

I. INTRODUCTION

Certain large area conjugated macrocyclic compounds have been shown to form a mesophase in a limited temperature range where it is energetically favourable for the molecules to stack face to face. The intermolecular separation along the stack is about 3.5 Å with some small variation along the stack which confers the liquid crystalline properties upon the material. The stacks form on a regular lattice typically hexagonal close packed and the molecules have some limited mobility between stacks. Such mobility allows a self healing process to limit the effect of defects. When this is

---

* Corresponding author. E-mail: k.scott@qmul.ac.uk

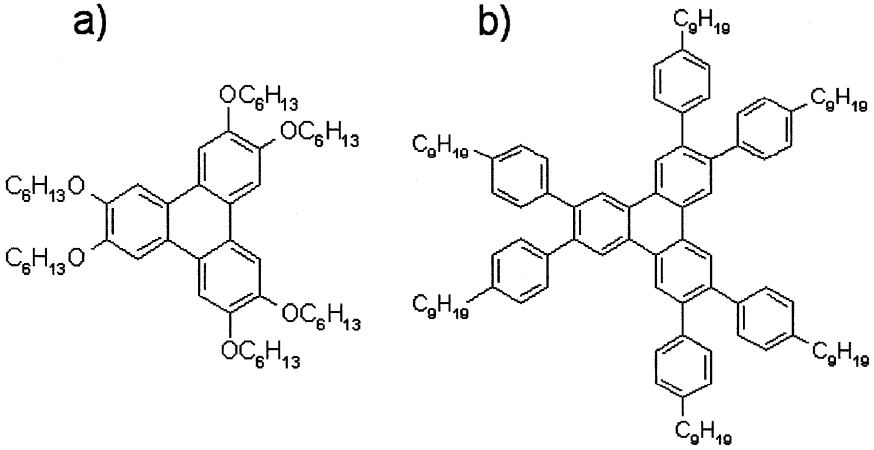

FIGURE 1 The structure of the discotic molecules (a) **HAT6** and (b) **PTP9**.

coupled with the proximity along the stack of conjugated electronic systems there is opportunity to achieve improved electronic transport properties. Because of this they have generated a great deal of interest and their electronic transport properties have been the subject of much study. The prototype discotic is the triphenylene molecule 2,3,6,7,10,11-Hexakis(hexyloxy)-triphenylene, **HAT6** shown in Figure 1a, whose properties have been reported in a number of papers [1,2,3,]. More recently it has been shown that mixing **HAT6** with an extended core aromatic discogen 2,3,6,7,10,11-Hexakis-(4-n-nonylphenyl)-triphenylene, **PTP9** shown in Figure 1b, results in a greatly increased hole mobility and range as a result of extra order conferred on the columnar structure [1].

II. EXPERIMENTAL

II.a. Sample Fabrication

Electrode cells were fabricated, as described previously for time of flight transit experiments [1], by evaporating semitransparent aluminium onto quartz slides. Two slides are placed on top of one another in a cross configuration, being separated by teflon spacers of approximately 5 μm thus creating a channel of well defined thickness. The slides were held in an assembly allowing temperature control. By melting the compound at the entrance to the channel the cell fills by capillary flow. The sample is then allowed to cool to the discotic mesophase. In this geometry the molecules self assemble in the mesophase, as stacks with the molecular stack axis perpendicular to the two electrodes. The thickness of the cell, $\boldsymbol{d}$, and its uniformity during assembly was monitored using interference fringes and measurement of the interference transmission spectrum using a Hitachi U3000 spectrophotometer. In this way the uniformity in thickness across a sample of several mm^2 in area could be kept to within better than 10%.

For optical absorption data cells were made slightly differently. Again two quartz slides were use but in this case without any metallic electrodes. Due to the high optical density of the samples sub micrometer gaps (0.5 μm) had to be used. To achieve this silicon monoxide spacers were evaporated onto one of the slides. The thickness of the cell was then measured as before and loaded with material. Optical absorption data was taken with the spectrophotometer at room temperature.

II.b. Dc Photoconduction Experiments

DC photocurrents were measured using a 610C Keithley electrometer in normal current mode. An electric field, $\boldsymbol{E}$, was applied across the sample by applying a potential difference, V, between the electrodes. After an electric field is applied the dark current is allowed to reach a steady value over time before the sample is illuminated. The photocurrents were allowed to settle for approximately 10 minutes before each reading was taken. During this procedure the output of the electrometer was displayed on a Philips PM8251 chart recorder, which allows the steady state photocurrent and dark current to be easily determined.

The light source used for DC photocurrent measurements was a 500 W Xenon lamp coupled with a Monospek 1000 monochromator (1 m focal length) with a 1200 lines/mm grating. The input and output slits were kept at 1.5 mm to give a resolution $\Delta\lambda \approx 1$ nm. The light intensity of the output was measured using a photodiode of known responsivity $R(\lambda)$. In this way the data was normalised to the number of photons incident upon the sample.

This technique of obtaining DC photocurrents and quantum efficiencies has been used previously on thin films of polydiacetylenes, and is describe in more detail there [4].

III. PHOTOCONDUCTION OBSERVABLES

DC photocurrents measure the generation efficiency for photocarrier production. This quantity is generally compounded with the carrier range against recombination, $\boldsymbol{s}$.

$$I_{DC} = e\eta\phi\dot{N}A\frac{s}{d} \tag{1a}$$

Where η is the primary quantum efficiency for creating electron hole pairs and ϕ is the probability that photogenerated carrier pairs avoid geminate recombination, and contribute to the subsequent photocurrent. $\dot{N}$ is the rate at which photons are absorbed per unit area, A is the sample active area and d is the electrode separation.

To find the generation efficiency, $\{\eta\phi\}$, it is necessary to have some complementary knowledge of s. In the experiments described here the sample geometry has been created such that the photocarriers are all created close to the illuminated electrode. If a distinctive transient photocurrent $I(t)$ is seen, after pulsed illumination, where the current falls rapidly after a transit time across the sample thickness. It is possible to equate s with d and Eq. (1a) now becomes

$$I_{DC} = e\eta\phi\dot{N}A \tag{1b}$$

Such experiments have been reported previously for both **HAT6** [5] and **HAT6:PTP9** [1] and transits are only found for holes and in the case of **HAT6** only in the mesophase. Equation (1b) is then valid provided no linear Shockley Read recombination or bimolecular recombination is present. There is now the opportunity to find an absolute measure of $\{\eta\phi\}$.

IV. RESULTS

Figure 2(a) shows the temperature dependence of $\{\eta\phi\}s/d$ for **HAT6** at a high and a low electric field. The sample has $d = 5\,\mu\text{m}$. The measurements were made using DC photocurrents at 337 nm and analysed using Eq. (1a). Also shown are the crystalline/discotic/isotropic phase boundaries. In the discotic phase there is a hole transit and $s = d$. In this phase the abscissa shows the value of $\{\eta\phi\}$. At the crystalline/discotic phase boundary there is an abrupt decrease in the DC photocurrent as s dramatically decreases in the crystalline phase where no hole transit occurs. The related trapping of charge in the crystalline phase has been demonstrated previously in time of flight transient photoconduction experiments [5].

For the 50:50 binary mixture **HAT6:PTP9**, temperature dependence of $\{\eta\phi\}$ at 337 nm is plotted in Figure 2(b), $s/d = 1$ since holes have been demonstrated to transit the sample in both the discotic and glassy phase, in previous transient photoconduction experiments [1]. Here it should be noted that there can be a large error associated with the photocurrents of the mixture, due to the combination of large dark current in the **HAT6:PTP9** and the lower quantum efficiencies, compared to the **HAT6**.

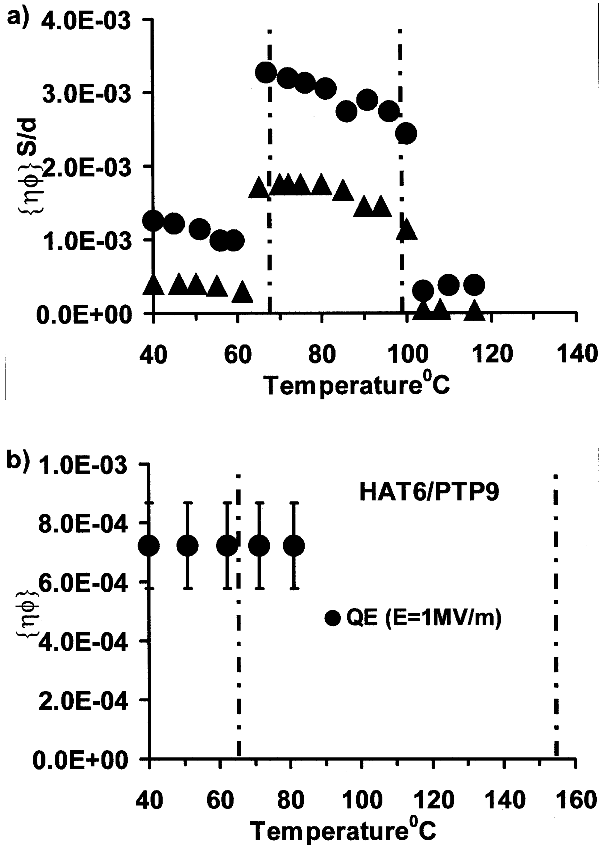

FIGURE 2 (a) Dependence of $\{\eta\phi\}S/d$ on temperature for **HAT6** at applied electric fields of 1 MV/m ● and 0.1 MV/m ▲. The vertical dashed lines show the crystalline/discotic/isotropic boundaries at 70°C and 100°C. Figure 2 (b) Dependence of $\{\eta\phi\}$ on temperature for **HAT6:PTP9** at an applied electric field of 1 MV/m ●. The vertical dashed lines show the glassy/discotic/isotropic boundaries at 66°C and 155°C.

Figure 3(a) shows the wavelength dependence of $\{\eta\phi\}$ for a 5 μm **HAT6** sample in the discotic phase at a temperature of 61°C. Also shown is the optical absorption spectrum of a **HAT6** sample of 0.61 μm thickness in the crystalline phase at room temperature.

Figure 3(b) shows the corresponding data for the binary mixture of **HAT6:PTP9**.

The photoaction spectra were taken at the same temperature of 30°C at which the optical absorption spectrum shown was obtained.

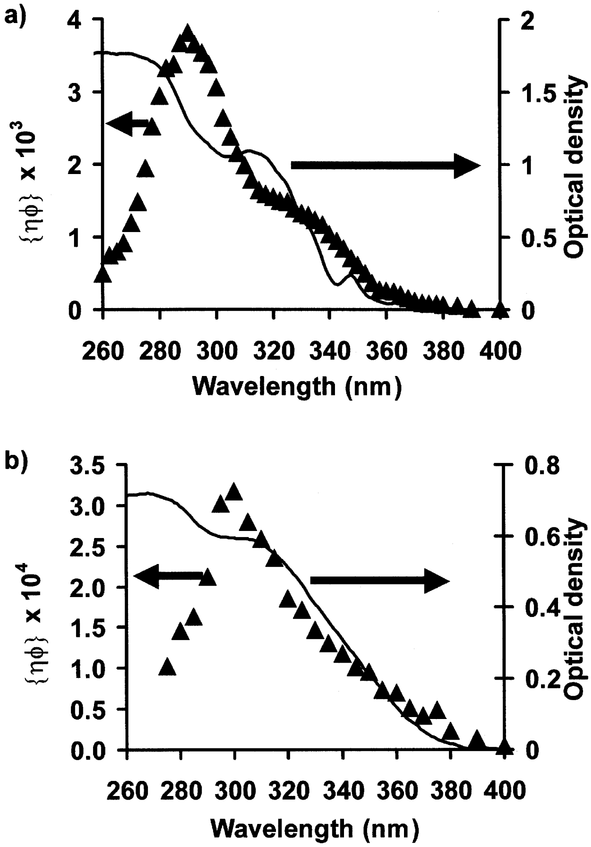

FIGURE 3 (a) The dependence of $\{\eta\phi\}$ ▲ with wavelength of **HAT6** in the discotic phase at 61°C, the absorption spectrum (solid line) is also shown. Figure 3 (b) The dependence of $\{\eta\phi\}$ ▲ with wavelength of **HAT6:PTP9** at 30°C, the absorption spectrum (solid line) is also shown.

V. DISCUSSION

The main observation when comparing the generation efficiencies of the two materials is that the **HAT6:PTP9** mixture shows a reduction of approximately a factor of 4 to that of **HAT6** in the discotic phase, at an electric field of 1 MV/m, where $\{\eta\phi\}$ changes from 3×10^{-3} to 7×10^{-4}.

For **HAT6** if the values of $\{\eta\phi\}$ ***s*/*d*** are compared just either side of the phase boundary it is possible to get a value for ***s*/*d*** by assuming that $\{\eta\phi\}$, which is known in the mesophase, does not change abruptly at the boundary. Since ***d*** is the electrode separation and known, a value for ***s*** may thus be calculated. In Figure 2(a) the value of ***s*** is 2 μm and 1.1 μm at the two electric fields of 1 MV/m and 0.1 MV/m respectively. The carrier range ***s*** in the crystalline phase for **HAT6** is found to change from sample to sample and with the rate at which the sample temperature is lowered into the crystalline phase from the discotic phase. We believe that it is this effect that has caused ***s*** to differ in the two experiments. More careful control of the cooling rate will be used in future experiments. All of this seems to suggest that ***s*** is a measure of the quality and the number of defects frozen in to the columnar stacks in the crystalline phase, since the self-healing of defects.

In the case of **HAT6:PTP9**, charge transits in the discotic and glassy phase are observed. In this case the structure is more ordered with alternation of large **PTP9** and smaller **HAT6** molecules along the stack. This alternation of molecules forming an *ABABA*– stack is the most probable structure proposed from the analysis of low angle X-ray diffraction data [6] and modelling the molecule – molecule interactions using the extended electron distribution method to calculate the interaction energy between the two molecules [6].

Electrochemical experiments are in progress to determine energies of the highest occupied molecular orbital (HOMO) and lowest unoccupied molecular orbital (LUMO) of the two molecules in solution. We may speculate that a **HAT6:PTP9** system with an alternating stack structure may result in band offsets, due to differing HOMO and LUMO levels for the **HAT6** and **PTP9** molecules. In such a system carriers created on the molecule which has the lower energy state may not able to overcome the energy barrier to the next molecule with a higher energy state as quickly as in a system of the single material with no energy barrier between the molecules. This longer lifetime of the carrier pair on one molecule may result in a more effective geminate recombination for carriers on that molecule and a consequent reduction in ϕ as observed.

Care will have to be taken in the interpretation of such data since there will be molecular interactions in the glassy, crystalline and discotic phases compared to the isolated states measured in solution in electrochemical measurements.

For **HAT6:PTP9** the data shown in Figure 2(b) shows temperature independent photocarrier generation. In 3D Onsager [7], a carrier, thermalising a distance from its twin under the influence of an external electric field ***E***, will have a probability of avoiding geminate recombination ϕ given by:

$$\phi = \left[1 + \frac{eEr_{kT}}{2kT}\right] \exp\left(\frac{-r_{kT}}{b}\right) \tag{2}$$

where ***b*** is the thermalisation length and $\boldsymbol{r_{kT}} = \boldsymbol{e^2/4}\pi\varepsilon\varepsilon_0\boldsymbol{kT}$, is the coulomb radius, with ε being the relative permittivity and ε_0 is the permittivity of vacuum. It is obvious from Eq. (2) that if Onsager is to be applicable there must be an activation energy associated with the photocurrent.

The errors associated with the **HAT6:PTP9** data may hide some temperature dependence. By taking the very extreme case associated with the data errors and calculating the activation energy it is possible to obtain a value of $\Delta E \leq 90\,\text{meV}$. In the case of **HAT6** where accurate data is obtained, if the temperature dependence is examined in the same way in the discotic region only, an energy of 60 meV is obtained, but it has the wrong sign for an activation energy i.e. a decrease of photogeneration with increase in temperature.

In summary there is clearly no activation for **HAT6** and for **HAT6:PTP9** there is no clear evidence for any activation and only by analyzing an extreme interpretation of the data can a small activation be found.

The shape of the photoaction spectra for both the **HAT6** and **HAT6:PTP9** have the same form. They begin at long wavelengths by following the optical absorption and then show a rapid decrease after approximately 300 nm. One possible explanation for the drop in photogeneration efficiency could be that photon absorption below 300 nm creates a non-ionising species that remains neutral in the applied electric field and steals oscillator strength from the photocharge producing transition i.e. a branching ratio between the ionising state and a strongly bound exciton. Given the similarity of the action spectra it seems evident that the **HAT6** molecule is mainly responsible in the mixture for producing the photocarriers. On closer inspection of the two photoaction spectra it is seen that the whole **HAT6:PTP9** spectra is shifted by 10 nm to longer wavelengths, this may be explained by orbital mixing of the two molecules causing a shift in the bandgap of the **HAT6** molecule.

VI. CONCLUSIONS

Some workers [8] measuring photocurrents on **HAT6** have concluded that an Onsager type mechanism is appropriate to describe the generation process. However for 3D Onsager geminate recombination to be the determining factor in carrier generation requires that $\{\eta\phi\}$ is activated. The results shown here show no evidence for this in **HAT6:PTP9** and a contrary behaviour in **HAT6**. We would therefore be led to conclude that the Onsager mechanism plays no important role in photocarrier production on the basis of temperature dependence. We have shown that in the crystalline phase of **HAT6** the carrier range, s, while being dependent on sample production is of order 1 μm. Both **HAT6** and **HAT6:PTP9** having almost identical photoaction spectra suggesting that it is the **HAT6** molecule which is associated with free carrier charge generation.

REFERENCES

[1] Kreouzis, T., Scott, K., Donovan, K. J., Boden, N., Bushby, R. J., Lozman, O. R., & Liu, Q. (2000). ***Chem. Phys.***, ***262***, 489.

[2] Boden, N., Bushby, R. J., Clements, J., Donovan, K. J., Movagar, B., & Kreouzis, T. (1998). ***Phys Rev B***, ***58***(6), 3063.

[3] Adams, A., Closs, F., Frey, T., Funhoff, D., Haarer, D., Ringsdorf, H., Schumacher, P., & Siememsmeyer, K. (1993). ***Phys. Rev. Lett.***, ***70***, 457.

[4] Donovan, K. J., Scott, K., Spagnoli, S., & Berrehar, J. (1999). ***Chem. Phys.***, ***250***, 61.

[5] Donovan, K. J., Kreouzis, T., Boden, N., & Clements, J. (1998). ***J Chem. Phys.***, ***109***(23), 10400.

[6] Boden, N., Bushby, R. J., Lozman, O. R., & Wood, A. (2000). ***Angew. Chem.***, ***39***(13), 2333.

[7] Onsager, L. (1938). ***Phys. Rev.***, ***54***, 554.

[8] Nakayama, H., Ozaki, M., Werner, W., Schmidt, F., & Yoshinio, K. (1999). ***Jpn. J. Appl. Phys.***, ***38***, L1038.